NEWBORN - NExt generation high poWer fuel cells for airBORNe applications

WP8 – Power Line

D8.3 - Simulation analysis report

Document ID	NE-WP8-SE-NO-DEL-800003
Revision	00
Date	2023-06-29
Sensitivity	Sensitive
Restricted to	N/A
Export Control	NONE
EC Category	N/A

Approval Table	Title	Name	Date and Signature
Prepared by	Authors	Julius Zettelmeier	29-Jun-2023 DocuSigned by: Julius Zettelmeier 5AFC1939AA70441...
Approved by	Work Package Leader	Florian Hilpert	29-Jun-2023 DocuSigned by: Florian Hilpert 0931EF6AD05A4B1...
Approved by	Configuration Manager	Dorin Maxim	29-Jun-2023 DocuSigned by: Dorin Maxim F97C03BE7952428...
Approved by	Technical Leader	Ondrej Kotaba	29-VI-2023 DocuSigned by: Ondrej Kotaba BEC376C9572A433...

Co-funded by the European Union

REVISION HISTORY

Revision	Date	Revision summary
00	2023-06-29	Initial issue

Table 1: Revision history

INTELLECTUAL PROPERTY

Section/Chapter/Item	Owning Entity	Nature of IP	Comments
Entire deliverable excluding background information	FHG, UON, PVS, HON, NIT, PCS, FAU	Shared Foreground	

Table 2: Intellectual property

TABLE OF CONTENTS

LIST OF FIGURES

LIST OF TABLES

1 INTRODUCTION

1.1 Objective

The objective of this document is to present the simulation results obtained during the development process of the power line simulation toolset for the NEWBORN project. A detailed description of the models is outlined in deliverable D8.2. Basis is the electrical topology architecture model developed in Task 8.1 shown in in Figure 1. Please refer to D8.1 for a detailed description.

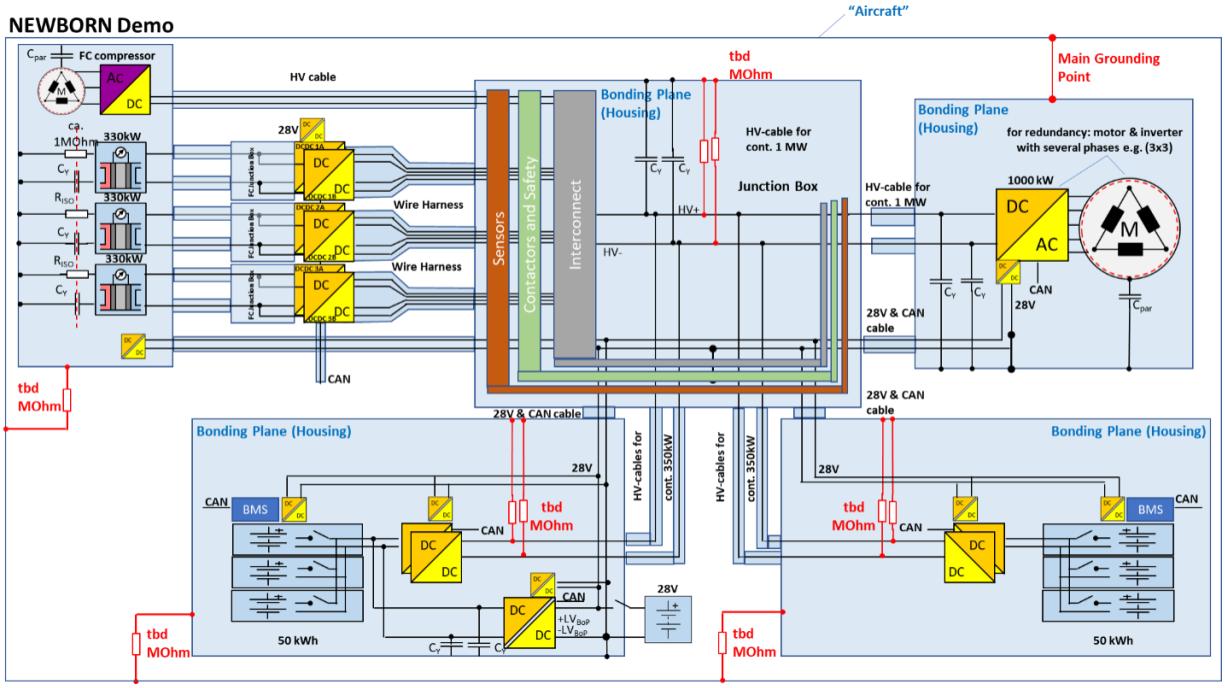

Figure 1: NEWBORN Demo electrical architecture from D8.1

1.2 Scope

The scope of this document is the functional modeling layer or fidelity that is relevant for basic architecture and topology studies discussed in deliverable D8.1. The behavioral layer will be discussed in detail in the next publication. First simulations regarding the behavioral layer have been conducted and are included within deliverable D8.1. First simulations are conducted for the purpose of demonstrating the capabilities of the developed tool and to support the discussions in Task 8.1.
A detailed analytic of the large and small signal stability of the HV-Bus will be covered by the next deliverable.
Power electronics modeling fidelities are summarized in Figure 2. Responsibilities for Friedrich-Alexander Universität (FAU) within the project lie at the functional and behavioral layer. Layer 4 will be covered within the development process of the power electronic converters and is therefore conducted by Fraunhofer-IISB (FhG) and University of Nottingham (UoN).
The purpose of the simulations is to confirm the function of the model, and the specific voltage levels don't fully represent the values chosen in D8.1. Please refer to D8.1 as a reference for them.
.

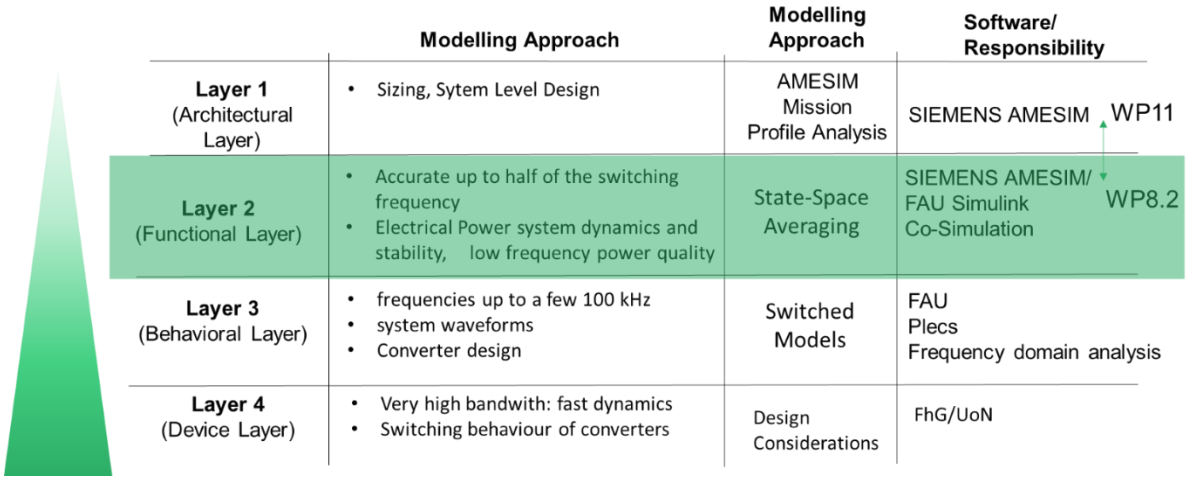

Figure 2: Power electronics simulation fidelities and modeling responsibilities within the NEWBORN project

To emphasize this subdivision, Figure 3 indicates the main phenomena occurring in the relevant frequency range for power electronic simulations. As stated above the objective of this report is to give an overview over the functional modeling fidelity closely linked to the control design.

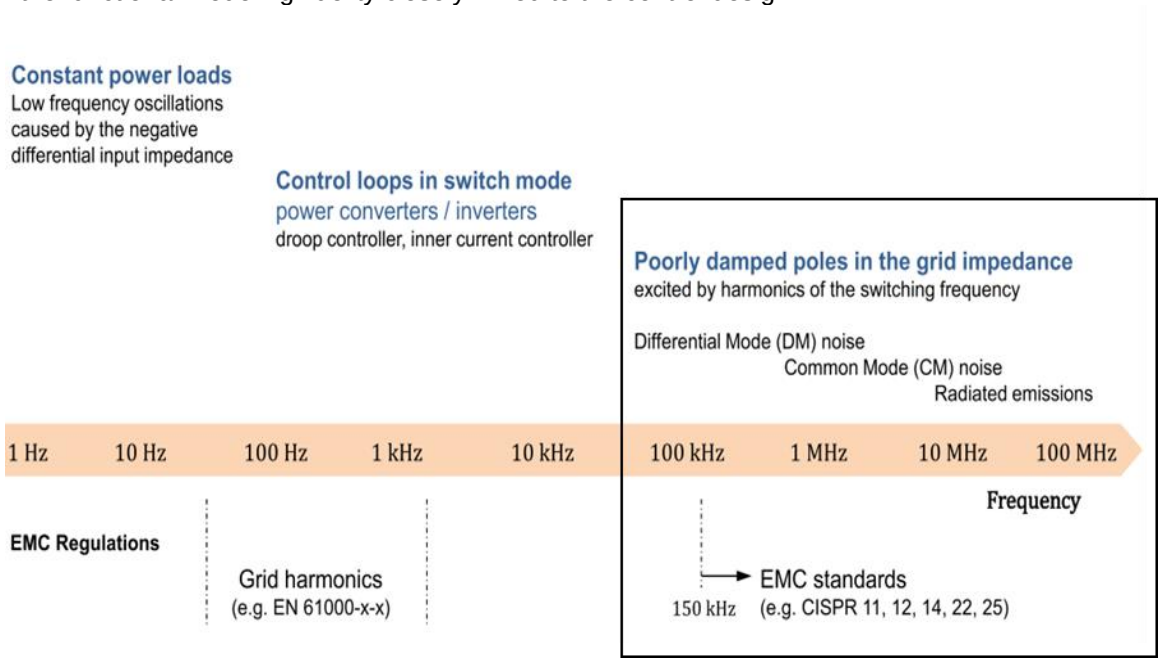

Figure 3: Phenomena within the frequency range in power electronics

2 MODEL OVERVIEW

Figure 4 gives an overview of the simulation developed simulation model. Please refer to deliverable D8.2 [3] for a detailed description of the models.

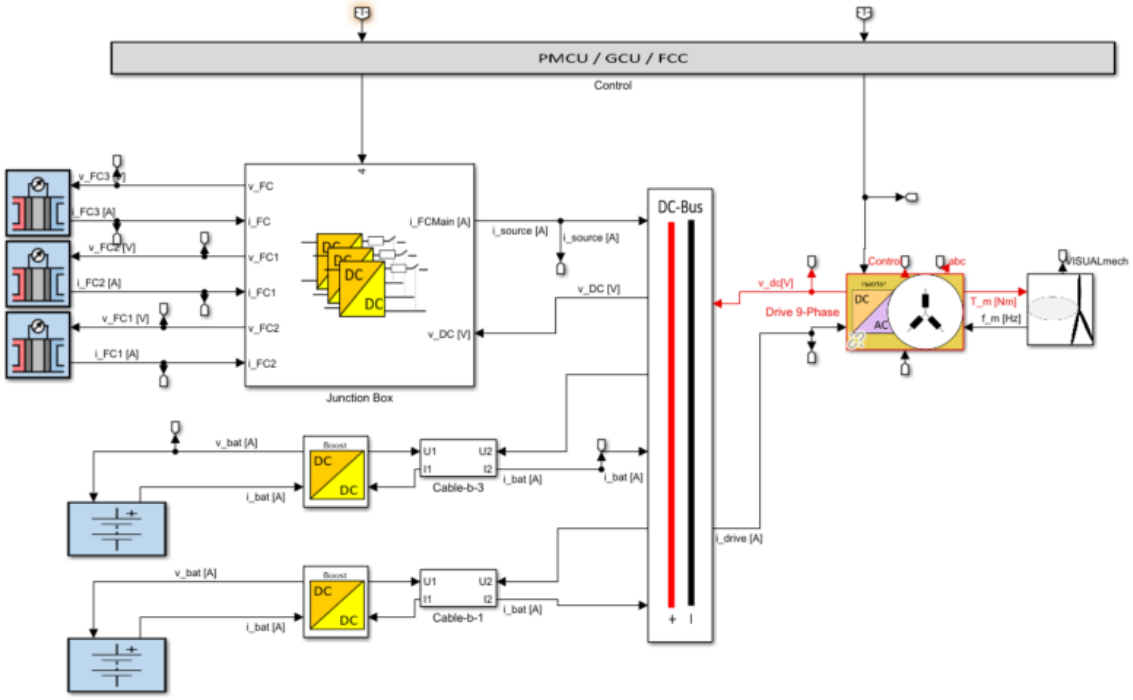

Figure 4: Simulation model developed (please refer to Deliverable D8.2)

Purely resistive connecting cables of 1mΩ (see D8.1 [1]) are used for the first simulation iteration presented here (Lumped cable model). In the final simulation report the influence of cable parameters such as inductances will be analyzed in detail. The respective modelling and parameterization will be integrated once data from Task 8.11 (HV Wiring, started in M6) is available.

3 DC VOLTAGE RANGES

In order to get an estimation about the HV-bus voltage levels during transients within the grid, the following simulation was conducted. Figure 5 provides the droop curves implemented for each of the fuel cell DC/DC converters and battery DC/DC converters respectively.

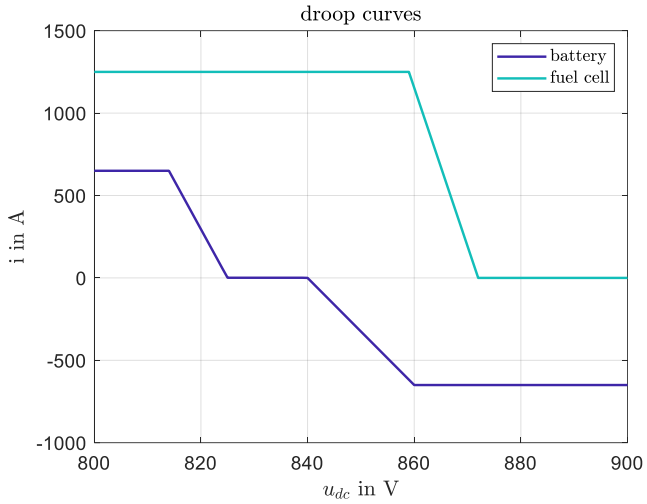

Figure 5: First iteration droop curves used during the DC Voltage level aspects

An ohmic load is used instead of the propulsion drive model shown in Figure 4 to obtain information about feasible voltage ranges in a best-case scenario considering droop control and the slow dynamics of the fuel cell.
Steps in the load (Figure 6) are assumed to analyse the effect of rapidly changing power demands. These will not be representative for the final NEWBORN demonstrator but will give an estimation about the achievable transients.

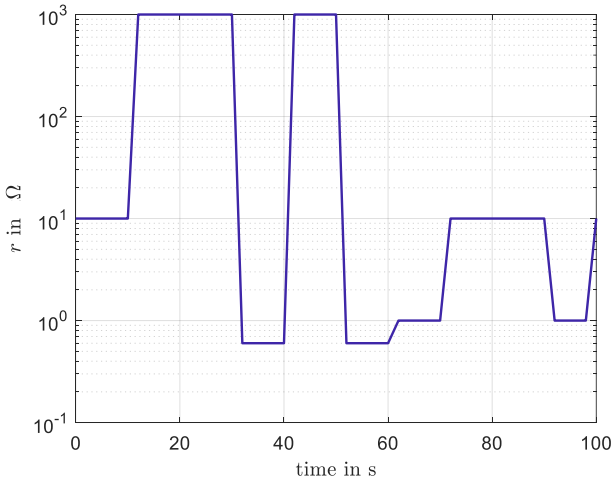

Figure 6: Ohmic resistance load profile used as a boundary condition

The capacitance on the output side of the converters will influence the dynamic behaviour of the system greatly [2]. Therefore, the total capacitance installed at the HV-Bus at the output side of the DC/DC converters has been considered as a parameter.

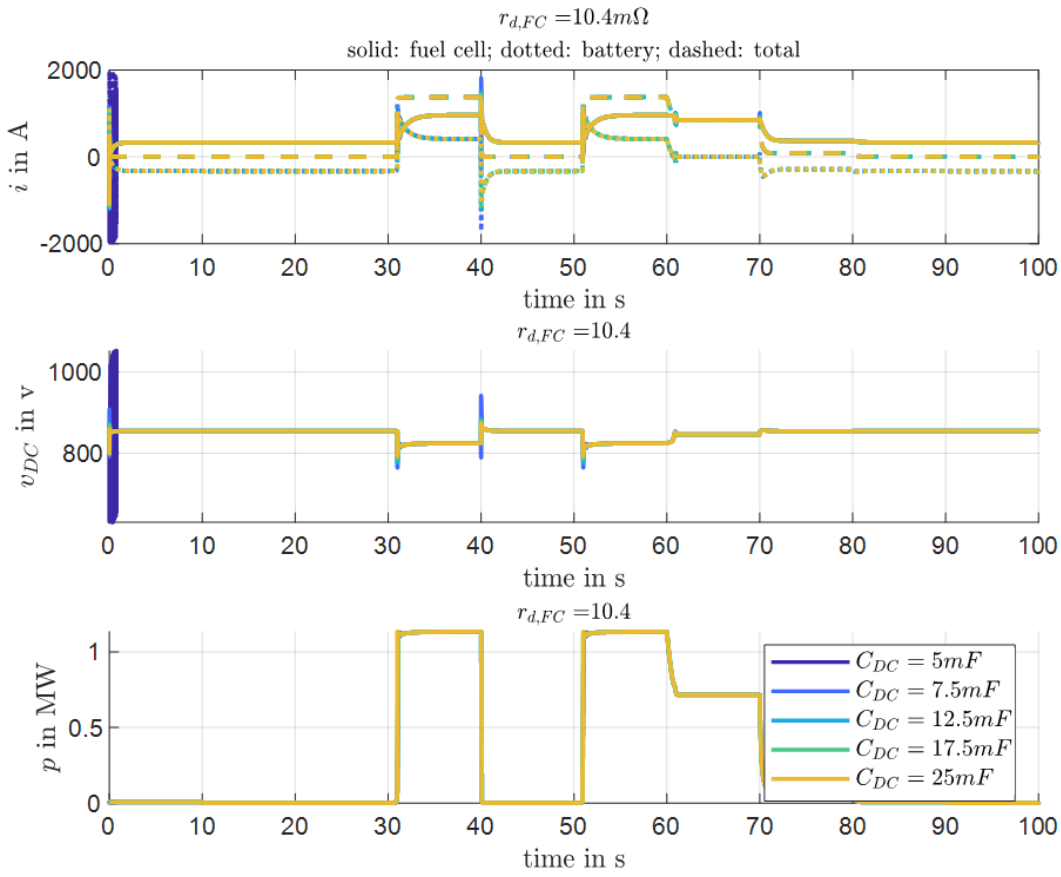

Figure 7: Simulation results for ohmic load profile analysis

Figure **7** gives an overview over the simulation results. Most critical load steps for the transient voltage behavior will be from 0W to 1MW and from 1MW to 0W. One can see the effect of the DC-Link capacitance C_{DC}. Instabilities occur for a capacitance of 5mF on the bus. It is worth mentioning at this point again that a detailed stability analysis based on impedance-based stability criteria and/or large signal Lyapunov theory based will be conducted in the upcoming months, accompanying the Power electronics component developments.

The following figures Figure **8** and Figure **9** show a magnification of the step to emphasize the dynamic effects occurring during the load steps.

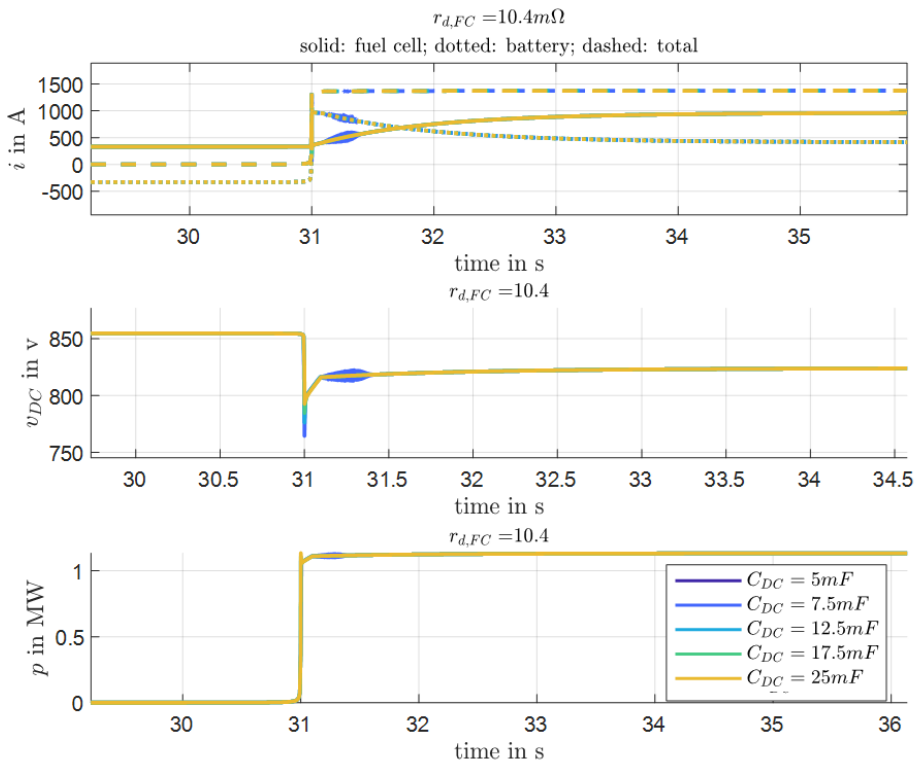

Figure 8: Magnification of the simulation results for ohmic load profile analysis

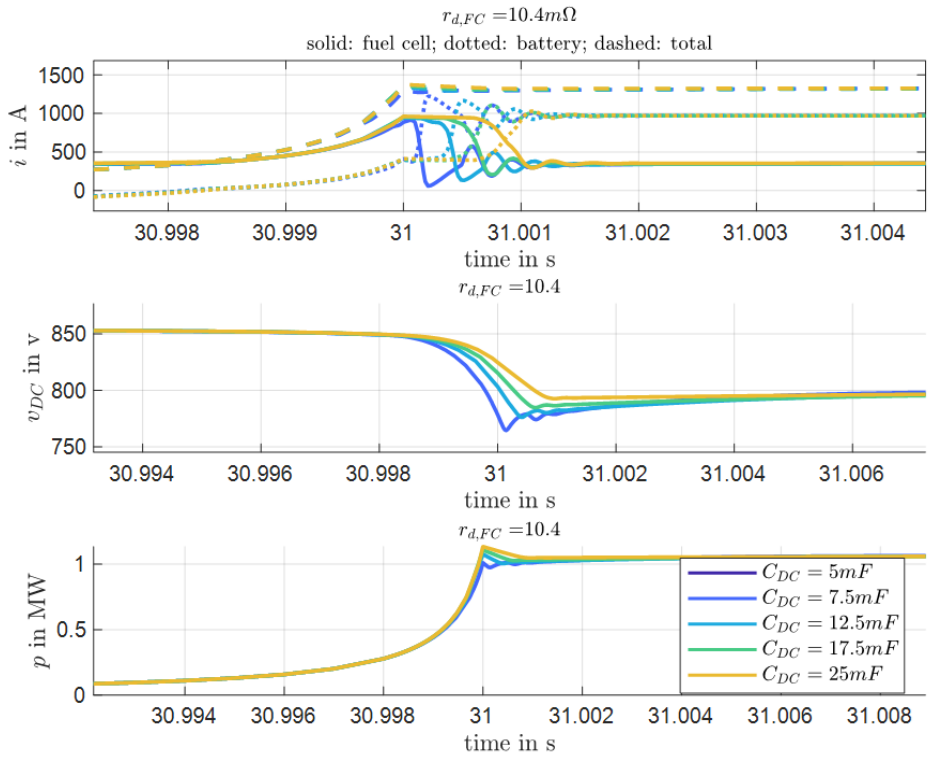

Figure 9: Second magnification of the simulation results for ohmic load profile analysis

From Figure **9** it can be seen that the current flowing to the load side (total current) is buffered by the fuel cell capacitances at the first incident. Because of the slow dynamics of the fuel cell, the current from the fuel cells will be falling to zero again afterwards.

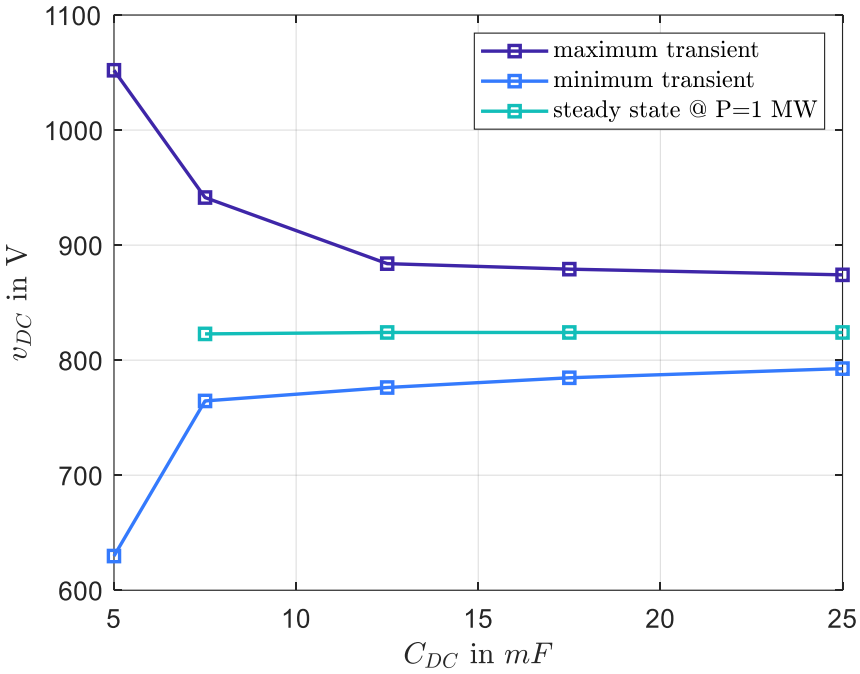

Figure 10: Processed simulation results

Figure 10 gives the processed results of the HV-Bus voltage v_{DC} as a function of the total DC-Link Capacitance on the source side of the grid. The transient maximum and minimum will level out at 12.5mF C_{DC} already at about 880 and 780V respectively. The steady state/ rated or nominal voltage is 825V.

4 MISSION PROFILE ANALYSIS (HOP)

The mission profile defined in deliverable D8.2 [3] will be used to simulate an aircraft hop (climb phase of the aircraft). Figure 11 and Figure 12 summarize the aircrafts state during the defined phase of the flight that leads to the reference power (see deliverable D8.2 [3]).

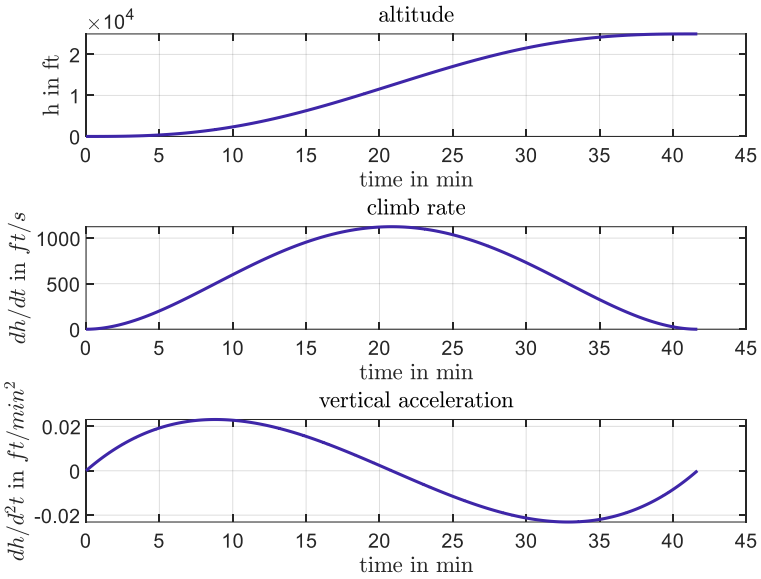

Figure 11: Trajectory Plan

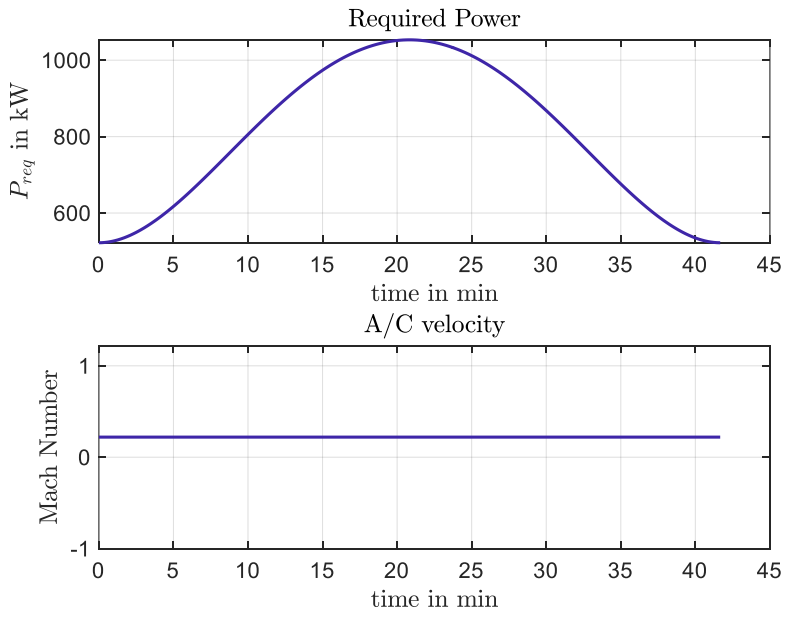

Figure 12: A/C Velocity and required power for the hop-trajectory

The above reference power profile P_{ref} is used for the following simulations. Furthermore, the DC Link capacitance is composed of 900µF for the inverter on the load side, and 5x3,5mF on the source side. Different droop control approaches will be analysed to evaluate their impact. All of these curves D1 to D4 are described in the following subchapters.

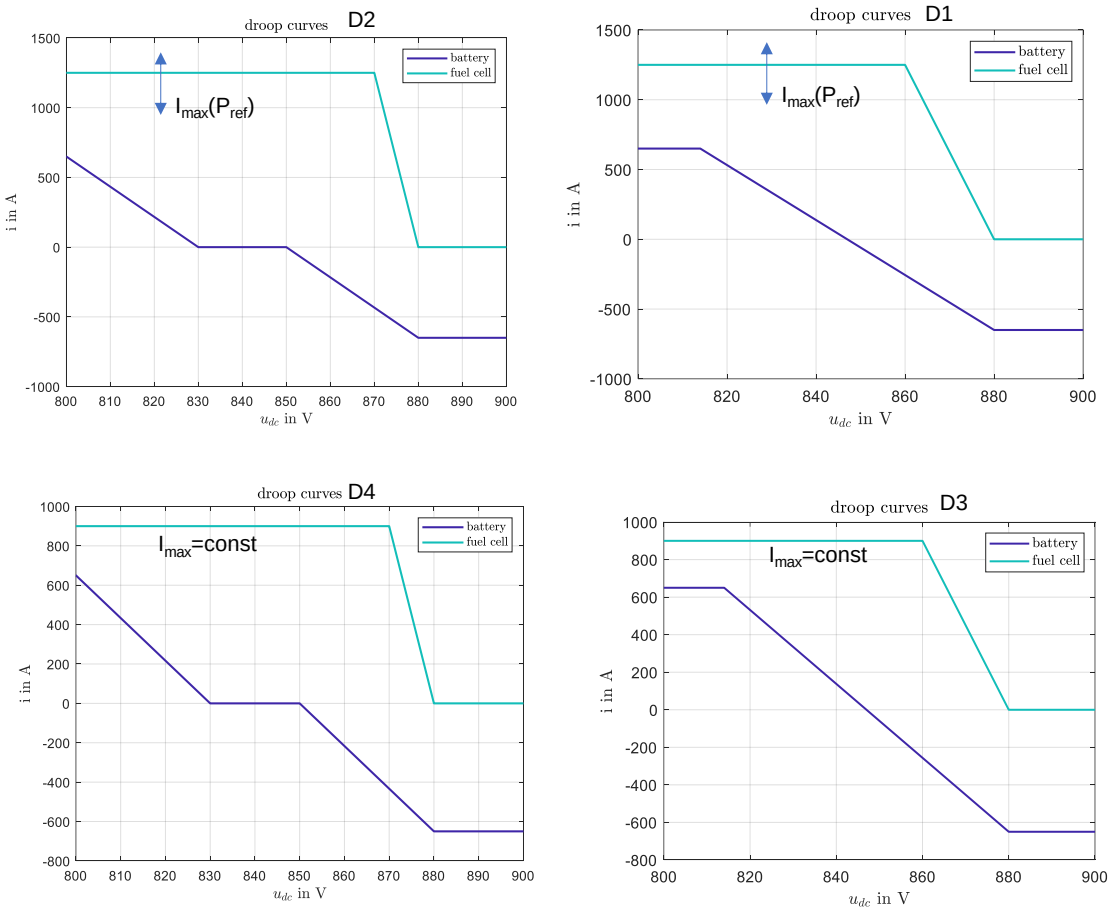

Figure 13: Analyzed droop curves for the mission analysis

4.1 Adaptive fuel cell operating points full/ battery droop (D1)

The first implemented droop curve (D1 - Figure 13). This will be defined as adaptive full droop as the maximum current of the fuel cell is calculated based on the current reference power and the battery droop curve does not include any horizontal characteristics within the nominal voltage operating range between 800V and 860V.

The following Figure 14 gives an overview over the resulting DC system states.

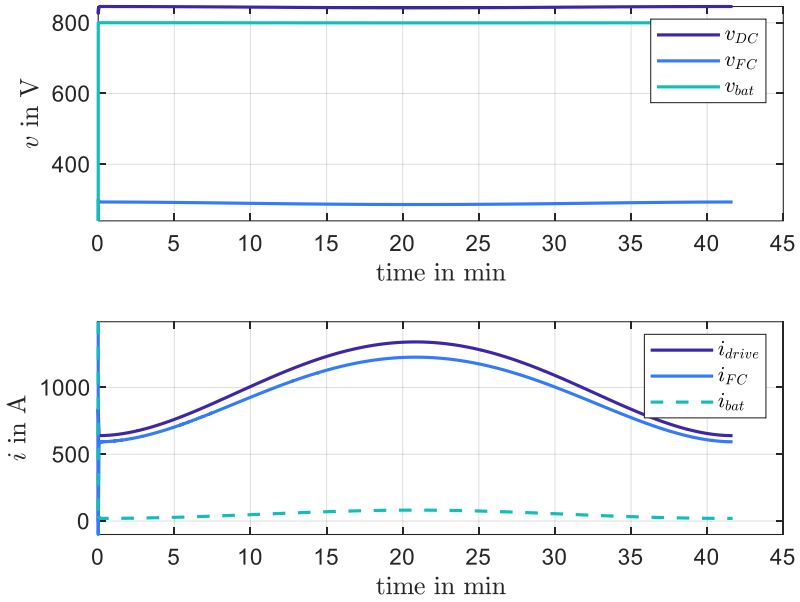

Figure 14: DC voltages and currents within the system

High compensating currents between the components/ capacitances in the incident of starting the system emphasize the necessity of pre-/ and discharge circuitry for the HV-DC Bus.

The DC link voltage is shown again magnified in the following Figure **14**, showing that stable operation is possible.

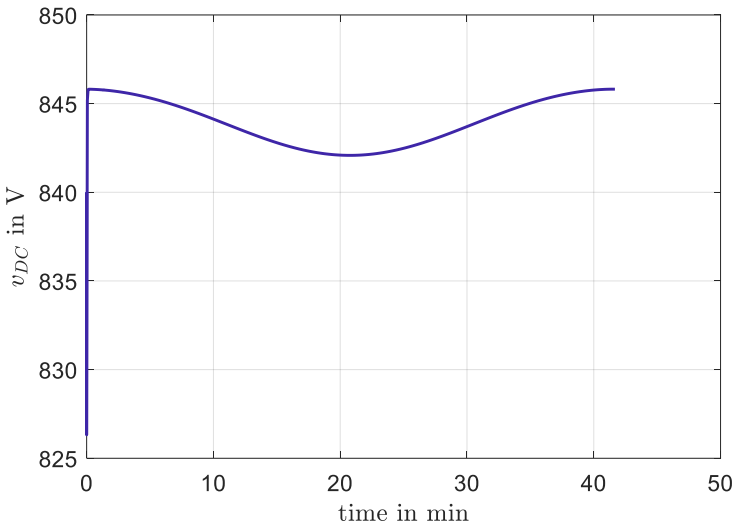

Figure 15: HV-Bus Voltage during

The following part shows the mechanical simulation results with the torque, rotor angle and speed of the motor or propeller (Figure 16) as well as the phase currents and voltages of the motor (Figure 17).

As can be seen, no saliency of the PMSM drive is considered (see D8.2 [3]), hence the reluctance torque is zero. The maximum torque is 1257 Nm at a constant speed of 8000 rpm. The phase currents amplitudes are 1550A at a voltage of 270V.

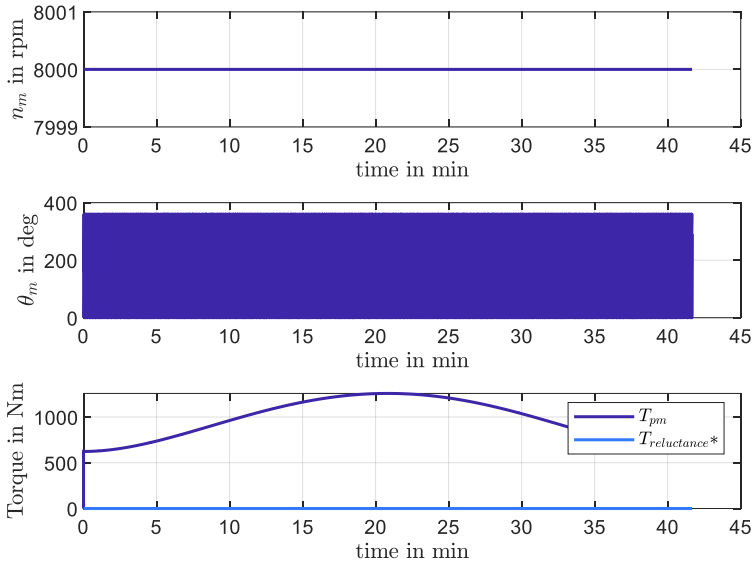

Figure 16: Mechanical simulation results ($T_{reluctance}$*: Reluctance torque due to saliency of the motor, θ_m: Rotor angle, n_m: mechanical speed of the rotor)

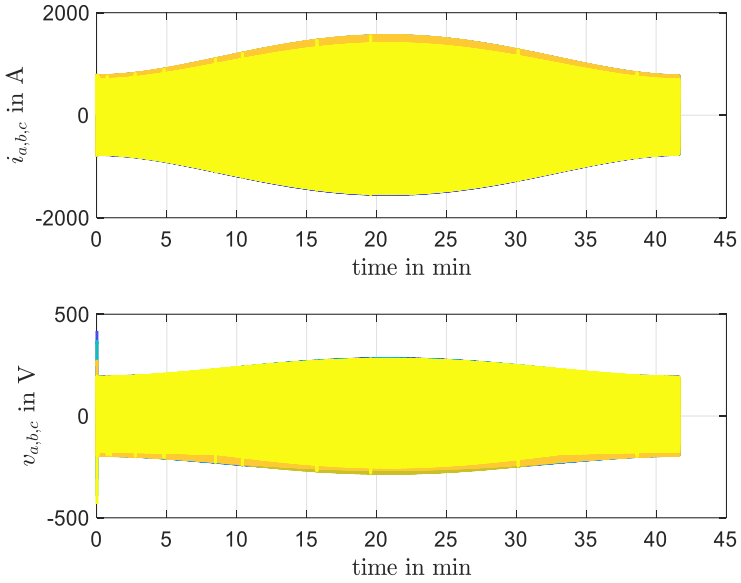

Figure 17: Envelopes of phase currents and voltages during the mission

In what follows, the power balance within the HV-grid is presented. As the demand from the fuel cell is adapted according to the current reference power, the fuel cell power is also adaptively manipulated. This leads to inefficient operation of the fuel cell.

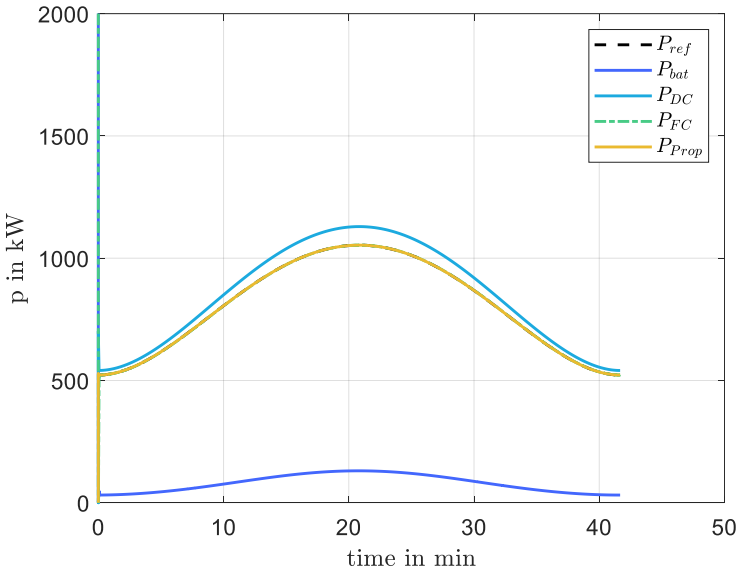

Figure 18: Power reference profile P_{ref} and resulting powers (P_{dc}: Power drawn from the DC-Grid, P_{prop}: shaft power, P_{FC}: Power provided by the fuel cell, P_{bat} : Power provided by the battery)

It is worth mentioning, that the battery and fuel cell powers are composed of the total sum of all fuel cell stacks (3) and battery modules (2).

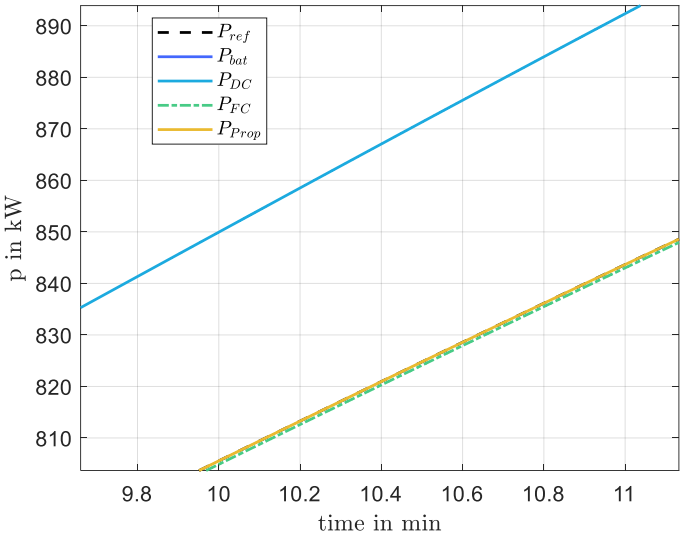

Figure 19: Magnification of the power results

The effect of losses within the inverter and motor is shown in Figure 19 by the inequality of the power P_{dc} and the power $P_{prop.}$ Further the power at the rotor shaft follows the reference power with good accuracy, but slight deviation (Figure **20**).

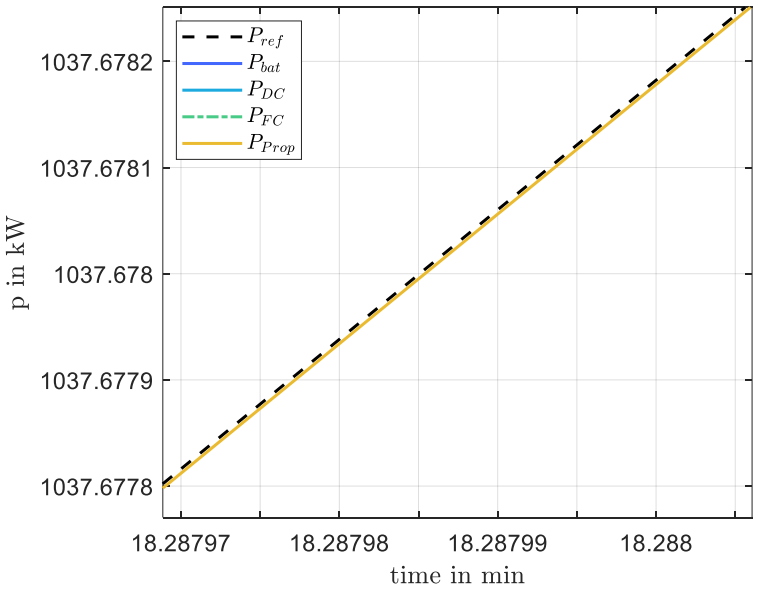

Figure 20: Second magnification of the power results

4.2 Adaptive fuel cell operating points/ interrupted battery droop (D2)

One can see from Figure **18**, that even at low power demands a current will be drawn from the battery. To evaluate the impact of a battery droop current reference equal to zero within a voltage range of 830V to 850V, the droop curve D2 according to Figure **13** has been simulated. The relevant results are again listed in the following figures Figure **21**, Figure **22**, Figure **23** and Figure **24**.

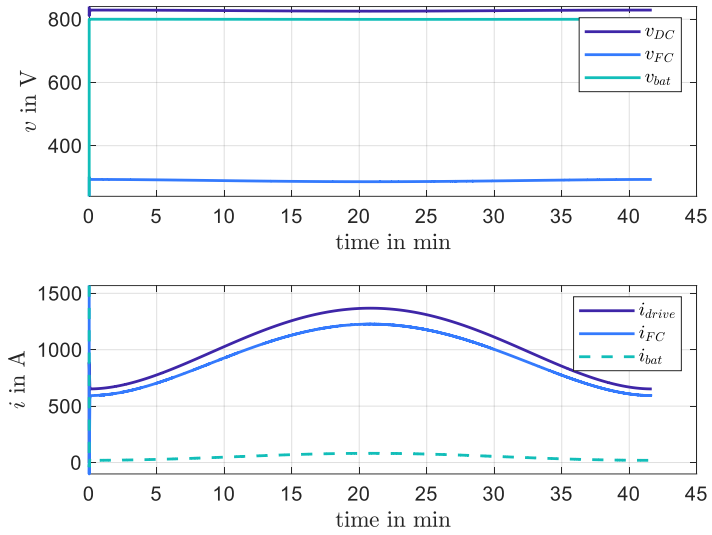

Figure 21: DC states in case of droop curve D2

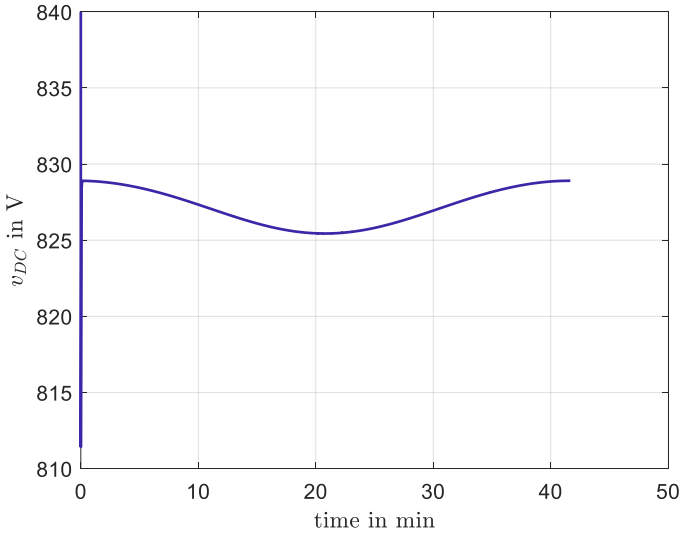

Figure 22: DC voltage in case of droop curve D2

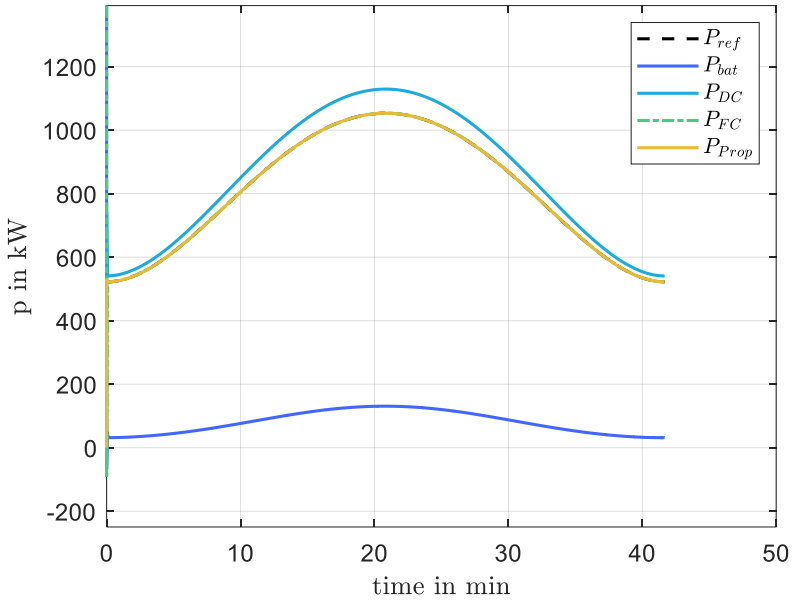

Figure 23: Power balance in case of droop curve D2

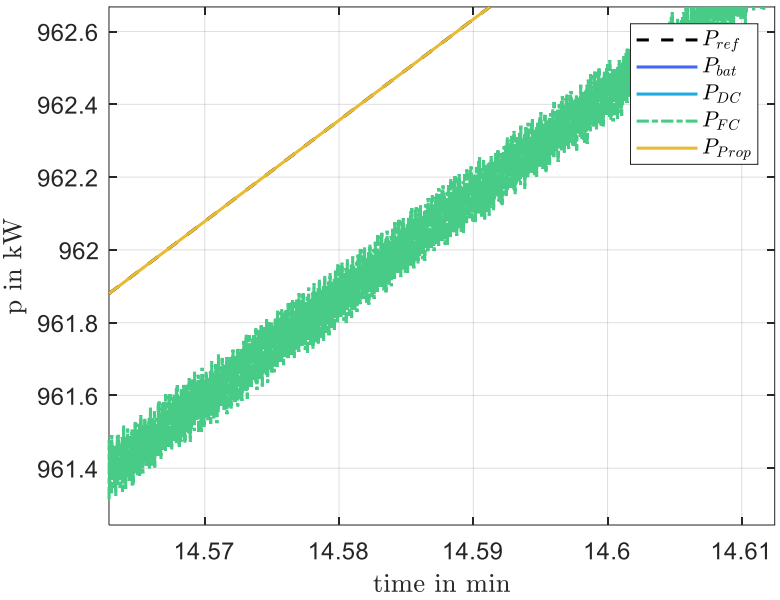

Figure 24: Magnified power balance in case of droop curve D2

The voltage v_{DC} system is stable. However, the lower droop curve region between 810V and 820V is in this case never left. Therefore, the battery will also in this case always feed in current. This emphasizes the necessity for a detailed analysis with different operating points of the HV-System, which shall be done later in the project. (e.g load dump scenarios, failures, etc.).

4.3 Constant fuel cell operating point/ full battery droop (D3)

As stated above, operating the fuel cell at changing operating points will lead to inefficiency of the system. Therefore, chapter 4.3 and 4.4 consider a fixed operating point, hence fixed maximum current of the fuel cell droop curve of 900A. The relevant results are again listed in the following figures (Figure **25**, Figure **26** and Figure **27**).

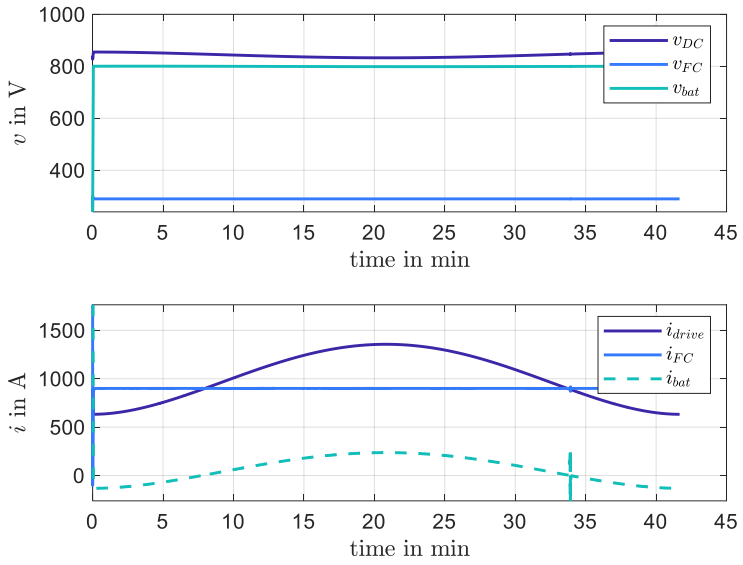

Figure 25: DC states in case of droop curve D3

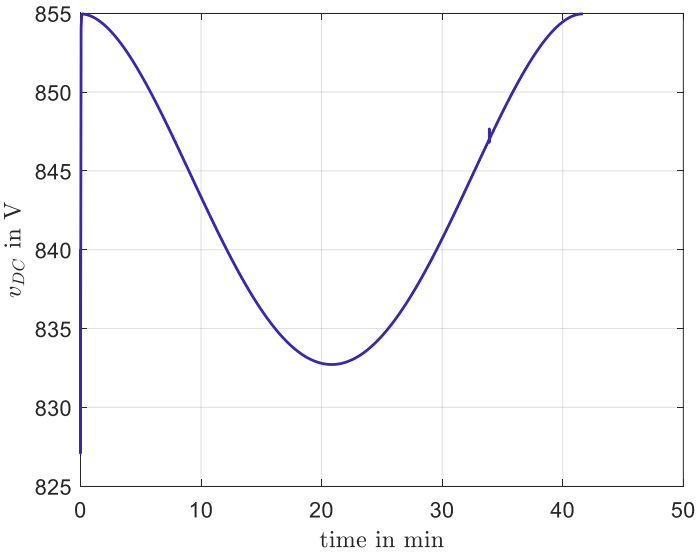

Figure 26: DC voltage in case of droop curve D3

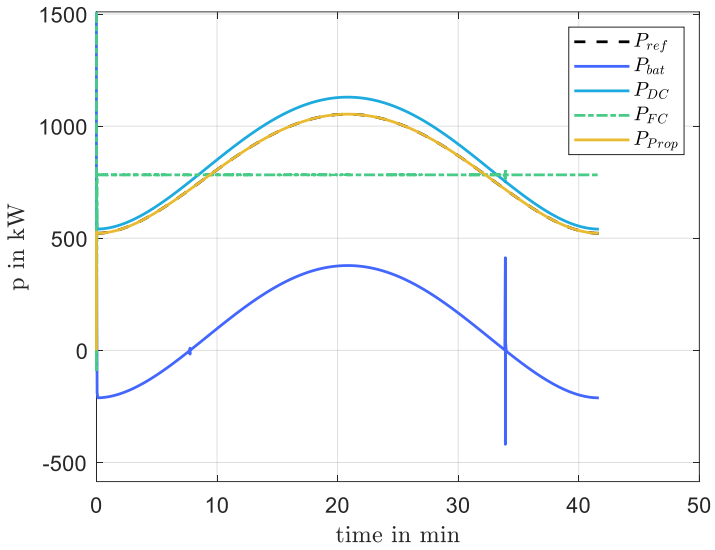

Figure 27: Power balance in case of droop curve D3

This configuration can also assure stable operation of the HV-DC bus. The fuel cell is operated at a constant power point as demanded (either maximum efficiency or maximum power), while the battery is providing the necessary power to stabilize the bus within the defined voltage range. A spike in battery current during the negative zero crossing at 34s can be seen which results from the point of discontinuity in the battery droop curve.

4.4 Constant fuel cell operating point/ interrupted battery droop (D4)

Lastly, droop curve D4 (Figure **13**) will give an indication about the behavior of the high voltage system with constant operating point of the fuel cell (900A) and of a battery droop current reference equal to zero within a voltage range of 830V to 850V.

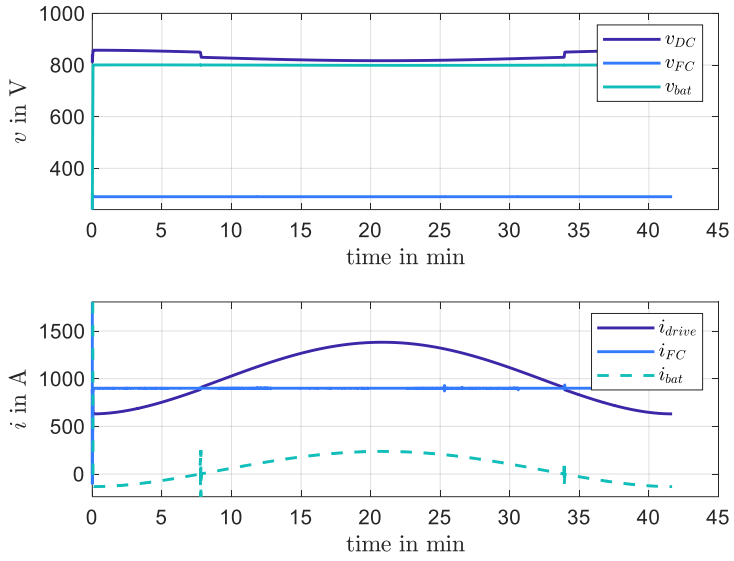

Figure 28: DC states in case of droop curve D4

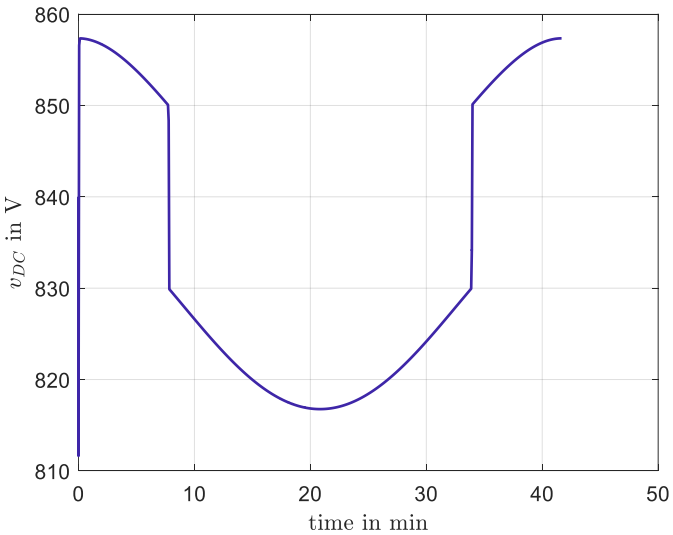

Figure 29: DC voltage in case of droop curve D4

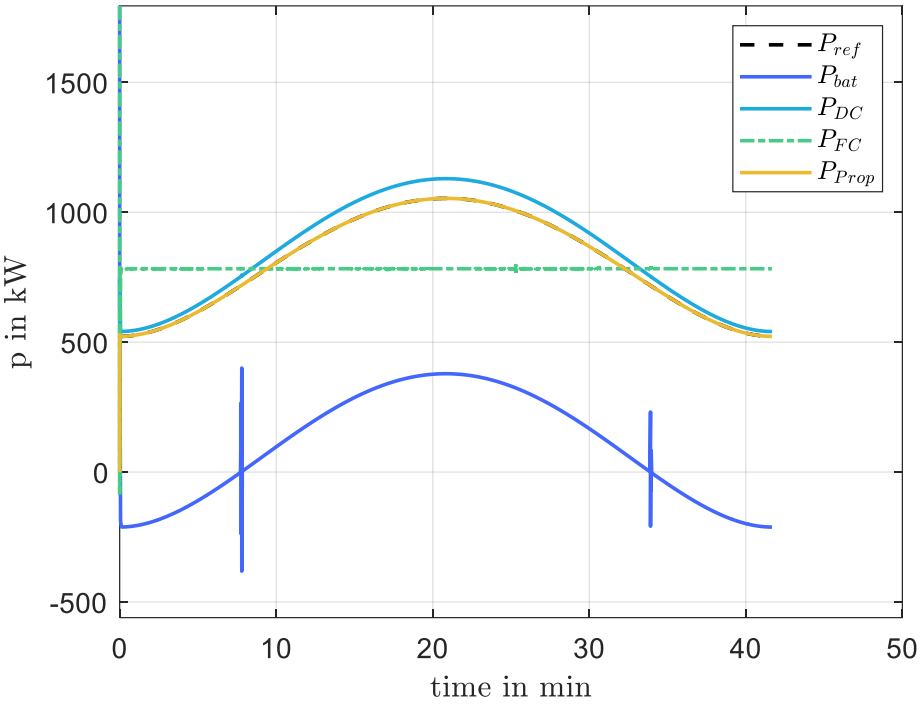

Figure 30: Power balance in case of droop curve D4

One can see fast slopes in the HV-DC voltage (dv/dt) v_{DC} voltage, when the battery droop reaches its zero sequence. This will most likely lead to EMI-problems in the HV system. A similar behavior is also expected for D2, but not visible in the simulation results from chapter 4.2 [2]. As a result, the interrupted droop curves D2 and D4 are not recommended.

.

5 EFFECT OF DC LINK CAPACITANCE ON STABILITY

The above simulation (chapter 3) considers an ohmic load to assess the transient behavior. In the following analysis, the complete system including the propulsion drive is analyzed. This can serve as a validation tool for the development of components, meaning DC/DC converters and the inverter, within the project. As the model incorporates modeled DC link capacitors as well as parasitics of the HV distribution system, interactive effects can be analyzed to optimize the individual power electronic components.

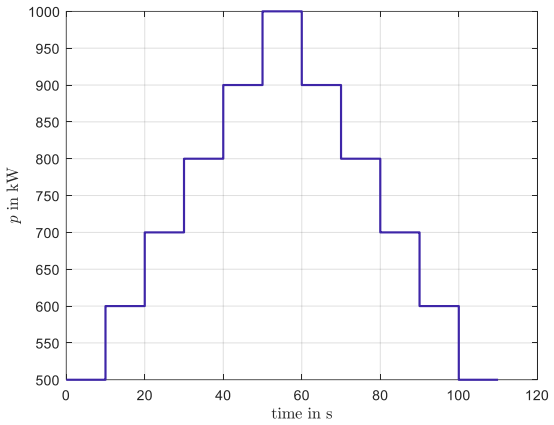

Figure 31: Reference power profile used

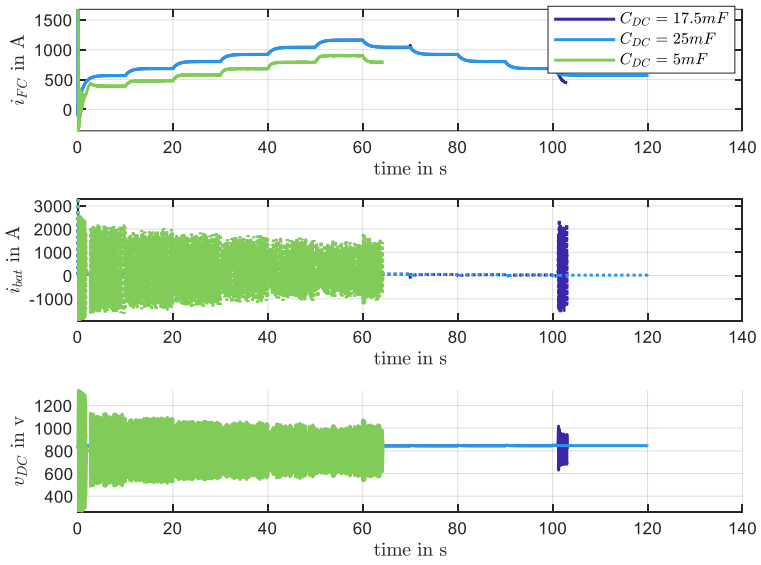

Figure 32: Simulation results

Clearly visible are instabilities at low DC-Link capacitance (green curve above), visualizing the capability to verify component design on system level. A detailed stability analysis of the entire NEWBORN system will be performed accompanying the individual power electronics component sizing.

5 CONCLUSION AND OUTLOOK

The initial simulation results presented here serve as functional verification of the complex electrical simulation model presented in the deliverable D8.2. The model is fully functional stable operation for different use cases of the model has been achieved.
More elaborate simulations for all operating points and failures will be performed as part of task 8.2, serving the individual component development throughout the ongoing project. A detailed stability analysis based on impedances or Lyapunov theory will be conducted. Droop curves like these presented in e.g. diagram D3 (Figure 13) are recommended and will be analysed. However, the current report does not consider defined charging of the battery, which will be part of future investigations. For that, the threshold for the fuel cell droop curve (Figure 13 - 860V) needs to be higher than the upper threshold of the battery droop curve (Figure 13 - 880V), with findings like these feeding directly into the control strategies of WP6.
Another aspect to be further investigated is the change of the droop curves to differentiable ones.

In general, even with the initial simulations performed, it can be stated that the voltage ranges defined within deliverable D8.1 [1] are feasible for the signal processing and control circuitry accuracy defined there.

6 REFERENCES

ID	Reference	Title	Revision
1	**Deliverable**	NE-WP08-SE-NO-DEL-8000010- D8.1 Electrical architecture & topology report	**0**
2	**Book**	Maerz, Martin (2022): Power Electronics for Decentral Energy Systems - Lecture Notes.	**0**
3	**Deliverable**	NE-WP08-SE-NO-DEL-800002 - D8.2 Simulation Model report	**0**

7 GLOSSARY

A/C	Configuration Management / Configuration Manager
HV	High voltage
DC	Direct Current
FAU	Friedrich-Alexander Universität
FhG	Fraunhofer-IISB
UoN	University of Nottingham
PC	Powercell
PVS	Pipistrel